NONLINEAR MHD STABILITY OF ALUMINIUM REDUCTION CELLS

V. Bojarevics, K. Pericleous
University of Greenwich, CMS, 30 Park Row, SE10 9LS, London, UK
(V.Bojarevics@gre.ac.uk)

Introduction. An industrial electrolysis cell used to produce primary aluminium is sensitive to waves at the interface of liquid aluminium and electrolyte. The interface waves are similar to stratified sea layers [1], but the penetrating electric current and the associated magnetic field are intricately involved in the oscillation process, and the observed wave frequencies are shifted from the purely hydrodynamic ones [2]. The interface stability problem is of great practical importance because the electrolytic aluminium production is a major electrical energy consumer, and it is related to environmental pollution rate. The stability analysis was started in [3] and a short summary of the main developments is given in [2]. Important aspects of the multiple mode interaction have been introduced in [4], and a widely used linear friction law first applied in [5]. In [6] a systematic perturbation expansion is developed for the fluid dynamics and electric current problems permitting reduction of the three-dimensional problem to a two-dimensional one. The procedure is more generally known as "shallow water approximation" which can be extended for the case of weakly non-linear and dispersive waves. The Boussinesq formulation permits to generalise the problem for non-unidirectionally propagating waves accounting for side walls and for a two fluid layer interface [1]. Attempts to extend the electrolytic cell wave modelling to the weakly nonlinear case have started in [7] where the basic equations are derived, including the nonlinearity and linear dispersion terms. An alternative approach for the nonlinear numerical simulation for an electrolysis cell wave evolution is attempted in [8 and references there], yet, omitting the dispersion terms and without a proper account for the dissipation, the model can predict unstable waves growth only. The present paper contains a generalisation of the previous non-linear wave equations [7] by accounting for the turbulent horizontal circulation flows in the two fluid layers. The inclusion of the turbulence model is essential in order to explain the small amplitude self-sustained oscillations of the liquid metal surface observed in real cells, known as "MHD noise". The fluid dynamic model is coupled to the extended electromagnetic simulation including not only the fluid layers, but the whole bus bar circuit and the ferromagnetic effects [9].

1. Shallow layer non-linear wave model. An aluminium electrolysis cell is a part of a row of similar cells, where each cell is connected in series to the neighbours by a complex arrangement of current-carrying bus bars shown in Fig. 1 for a particular case of 500 kA cells at the end of line. The electric current to the individual cell is supplied from above via massive anode bus bars made of solid aluminium, from which anode rods connect to the carbon anodes. The liquid electrolyte layer beneath the anode blocks is relatively poor electrical conductor of a small depth (4–6 cm) if compared to its horizontal extension (2–4×6–20 m). The electrolyte density is of little difference to the liquid aluminium pool created as the result of electrolytic reaction as the bottom liquid layer of depth 20–30 cm. For the "shallow water" approximation the horizontal dimensions L_x and L_y are assumed to be much larger than the typical depth H, and the interface wave

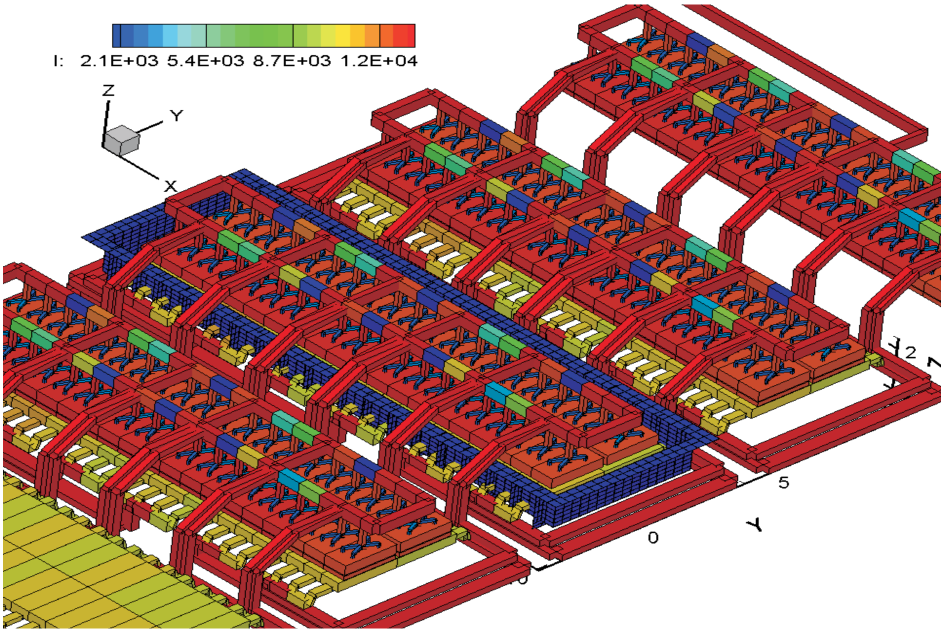

Fig. 1. 500 kA cell busbars and position of the cell in the row.

amplitude A is assumed to be small relative to the depth. Thus the two small parameters of the problem are the depth $\delta = H/L$ and the amplitude $\varepsilon = A/H$.

With the purpose to derive the Boussinesq equations for the wave motion we will need to estimate the terms in the full three-dimensional Navier–Stokes equations. According to the small depth assumption a stretched vertical coordinate and the nondimensional interface deformation of small amplitude are represented as

$$\bar{z} = z/(L\delta), \quad H_0/(L\delta) = \bar{H}_0 = \varepsilon\zeta(x, y, t)\,.$$

With these definitions the nondimensional fluid flow equations (continuity, horizontal momentum and vertical momentum) are respectively:

$$\partial_k u_k + \delta^{-1}\partial_{\bar{z}} w = 0 \tag{1}$$

$$\partial_t u_j + u_k \partial_k u_j + \delta^{-1} w \partial_{\bar{z}} u_j = -\partial_j p + \mathrm{Re}^{-1}(\delta^{-2}\partial_{\bar{z}}\bar{\nu}_e \partial_{\bar{z}} u_j + \partial_k \bar{\nu}_e \partial_k u_j) + E f_j \tag{2}$$

$$\partial_t w + u_k \partial_k w + \delta^{-1} w \partial_{\bar{z}} w = \delta^{-1}\partial_{\bar{z}} p + \mathrm{Re}^{-1}(\delta^{-2}\partial_{\bar{z}}\bar{\nu}_e \partial_{\bar{z}} w + \partial_k \bar{\nu}_e \partial_k w) + E f_z - \delta^{-1}\,, \tag{3}$$

where the summation convention is assumed over the repeating indexes k (equal to 1 or 2, respectively for x, y coordinates), ν_e is the nondimensional effective turbulent viscosity, f_j are the components of electromagnetic force, and the last term in (3) represents the constant gravity. The nondimensional governing parameters are the Reynolds number and the electromagnetic interaction parameter:

$$\mathrm{Re} = L u_0/\nu\,, \qquad E = (I B_0/L^2)/(\rho u_0^2/L) = I B_0/(L^2 \rho g \delta)\,.$$

The Boussinesq equations can be derived formally if representing the velocity as an expansion in the small amplitude parameter:

$$\mathbf{u}(x, y, z, t) = \mathbf{u}_0(x, y, t) + \varepsilon \mathbf{u}_\varepsilon(x, y, z, t) + o(\varepsilon)\,, \tag{4}$$

where $\mathbf{u}_0$ is the horizontal circulation, $\mathbf{u}_\varepsilon$ is the wave related velocity. An important feature of the shallow water approximation is the depth averaging procedure defined for the variables in each layer identified with number "i" . E.g., for the

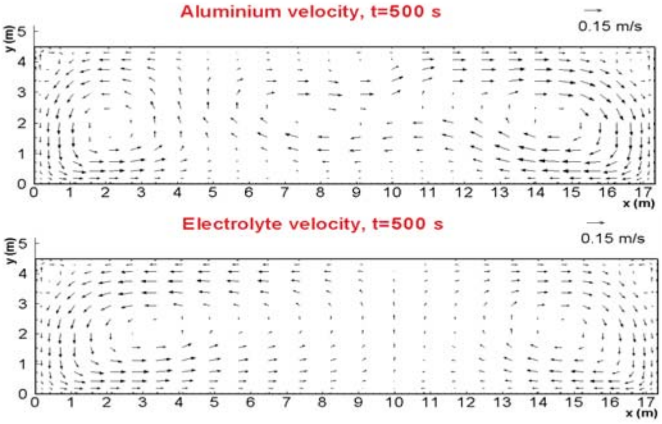

Fig. 2. Horizontal velocity in the two layers for the 500 kA cell.

horizontal velocity components the depth average is

$$\hat{u}_j(x,y,t) = \left(\bar{H}_i - \bar{H}_0\right)^{-1} \int u_j \, \mathrm{d}\bar{z}\,, \tag{5}$$

and similarly for other physical quantities. The same depth averaging procedure formally can be applied to the fluid flow equations (1)–(3). In this short communication we will present only the final equations. The depth average of the continuity equation (1) for each of the two fluid layers is

$$\varepsilon \partial_t \zeta = \partial_j \left[\left(\bar{H}_i - \varepsilon\zeta\right) \hat{u}_j \right], \tag{6}$$

which is accurate to all orders in ε and δ. When the depth averaging procedure (5) is applied to the horizontal momentum equations (2), the equations for the horizontal circulation $\mathbf{u}_0$ plus ε-order $\hat{\mathbf{u}}_\varepsilon$ wave motion: $\hat{\mathbf{u}} = \hat{\mathbf{u}}_0 + \hat{\mathbf{u}}_\varepsilon$ are

$$\partial_t \hat{u}_j + \hat{u}_k \partial_k \hat{u}_j = -\partial_j p(\bar{H}_0) - \varepsilon \partial_j \zeta - \mu \hat{u}_j + \mathrm{Re}^{-1} \partial_k \bar{\nu}_e \partial_k \hat{u}_{0j} + E \hat{f}_j - \frac{1}{2} \delta E \bar{H}_i \partial_j f_{0z} \tag{7}$$

where the continuity of the pressure at the interface is satisfied by introducing the pressure at the common interface. The nonlinear law for the friction at the top and bottom of the fluid layers is introduced in (7). Models for the friction coefficient $\mu(u,t)$ and the effective turbulence viscosity $\nu_e(x,y,t)$ will be described elsewhere. The equations of momentum (7) and continuity (6) for the two fluid layers can be combined in a single nonlinear wave equation for the interface $\zeta(x,y,t)$ by taking the time derivative of (6), the horizontal divergence of (7), and finally the difference between the resulting equations for the two layers to eliminate the common pressure at the interface $p(\bar{H}_0)$:

$$\begin{aligned} &\varepsilon \langle \rho/\bar{H} \rangle \partial_{tt} \zeta + \varepsilon \langle \mu\rho/\bar{H} \rangle \partial_t \zeta + \varepsilon \langle \rho \rangle \partial_{jj} \zeta = \\ &E \langle \partial_j \hat{f}_j \rangle - \delta E \left\langle \frac{1}{2} \bar{H} \partial_{jj} \hat{f}_z \right\rangle - \varepsilon \langle \rho/\bar{H} \partial_{tj}(\zeta u_{j0}) + \mu\rho/\bar{H} \partial_j(\zeta u_{j0}) \rangle - \langle \rho \partial_j (\hat{u}_k \partial_k \hat{u}_j) \rangle \end{aligned} \tag{8}$$

where $\langle F \rangle = F_1 - F_2$ denotes difference of the variable in the two layers.

2. Horizontal circulation effect on the waves. The equation (8) is formally a generalisation of the stability models used previously. By setting parameters $\varepsilon = \delta = 0$ the linear model is recovered [6]. In the following examples we will use the full electromagnetic model suitable for realistic cell simulations. The magnetic field is computed from the 5 cells in the same row (Fig. 1) and 5 cells in the return row (not shown). The cell is positioned close to the end of line in order to make it less stable and to generate small amplitude MHD sustained quasistationary oscillations. Further from the end of line the cell of the present design is absolutely stable. The velocity field is turbulent and time dependent. However the horizontal, depth averaged circulation reaches almost stationary distribution,

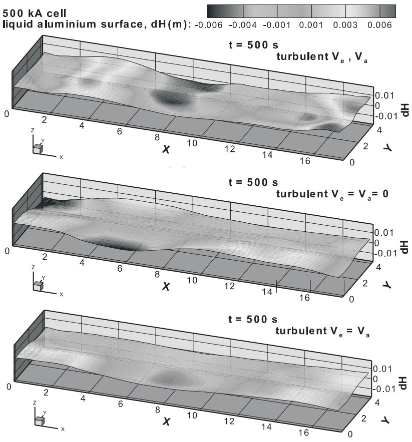

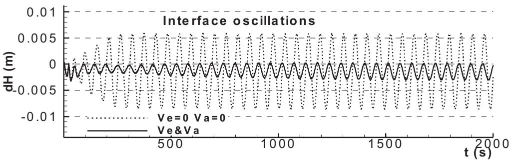

Fig. 3. Left: Interface at fixed time 500 s: including horizontal circulation (top), without horizontal circulation (middle), equal circulation in both layers (bottom). Right: Comparison of the interface oscillations: with and without the horizontal circulation effect.

which is different in each of fluid layers because of the electric current distribution variation. The horizontal electric current in the aluminium is responsible for the variation in the symmetric vortex structure, which is usually observed in the electrolyte layer (Fig. 2). The horizontal circulation vortices create a pressure gradient contributing to the deformation of the free surface. Typically an intense vortex is associated with a dip in its centre. For the two layers the effect on the common interface is in balance when two equal vortices are positioned one above the other because the last term in (8), responsible for the effect, is approaching zero as the densities of the two fluids are very close. Instructive comparisons can be made for the interface at the same time moments if accounting for the horizontal circulation and without the effect. Fig. 3 (top) clearly shows the dips at the centre and the right side where the aluminium vortices are more intense, and an oscillating wave crest on the left where the electrolyte circulation is more intense. There is nothing like this in the case when the horizontal circulation effect in (8) is set to zero, Fig. 3 (middle). The corresponding self sustained oscillation pattern is shown in Fig. 3,right. The wave frequency is nearly the same in both cases, but the interface topology and the amplitude are quite different. The effect of the vortices can be eliminated almost completely also if making the vortices equal in both layers, Fig. 3 (bottom). In the latter case the additional pressure variation exerts a stabilising effect on the interface. This observation can be an important tool for the more stable cell design, particularly in the end of line position.

REFERENCES

1. Ch.C. Mei. *The Applied Dynamics of Ocean Surface Waves* (World Scientific, 1989).
2. R. Von Kaenel, J.P. Antille. Magnetohydrodynamic stability in alumina reduction cells. *Travaux*, vol. 23 (1996), no. 27, pp. 285–297.
3. N. Urata, K. Mori, H. Ikeuchi. Behavior of bath and molten metal in aluminium electrolytic cell. *Keikinzoku*, vol. 26 (1976), no. 11, pp. 573–600.
4. A.D. Sneyd, A. Wang. *J. Fluid Mech.*, vol. 263 (1994), pp. 343–359.
5. R. Moreau, J.W. Ewans. *Journal of Electrochemical Society*, vol. 131 (1984), no. 10, pp. 2251–2259.
6. V. Bojarevics, M.V. Romerio. *Eur. J. Mech., B/Fluids*, vol. 13 (1994), no. 1, pp. 33–56.
7. V. Bojarevics. *Progr. Fluid Flow Res.: Turbulence and Applied MHD*, AIAA (1998), Chapter 58, pp. 833–848.
8. H. Sun, O. Zikanov, B.A. Finlayson, D.P. Ziegler. The influence of the basic flow and interface deformation on stability of Hall-Herault cells. *Light Metals 2005*, TMS (2005), pp. 437–441.
9. M. Dupuis, V. Bojarevics. Weakly coupled thermo-electric and MHD mathematical models of an aluminium electrolysis cell. *Light Metals 2005*, TMS (2005), pp. 449–454.